(14) Russell, T. P. *J. Appl. Crystallogr.* **1983**, *16*, 473.
(15) Silvestre, C.; Cimmino, S.; Martuscelli, E.; Karasz, F. E.; MacKnight, W. J. *Polymer* **1987**, *28*, 1190.
(16) Strobl, G. R.; Schneider, M. *J. Polym. Sci., Polym. Phys. Ed.* **1980**, *18*, 1340.
(17) Strobl, G. R.; Schneider, M.; Voigt-Martin, I. *J. Polym. Sci., Polym. Phys. Ed.* **1980**, *19*, 1361.
(18) Van Krevelen, D. W. *Properties of Polymers*; Elsevier: Amsterdam, 1976.
(19) Porod, G. *Kolloid-Z.* **1951**, *124*, 83.
(20) Porod, G. *Kolloid-Z.* **1952**, *125*, 51.
(21) Porod, G. *Kolloid-Z.* **1952**, *125*, 108.
(22) Ruland, W. *J. Appl. Crystallogr.* **1971**, *4*, 70.
(23) Vonk, C. G. *Appl. Crystallogr.* **1973**, *6*, 81.
(24) Koberstein, J. T.; Morra, B. S.; Stein, R. S. *J. Appl. Crystallogr.* **1980**, *13*, 34.
(25) Herman, W.; Stein, R. S. *Bull. Am. Phys. Soc.* **1987**, *32*, 876.
(26) Popli, R.; Mandelkern, L. *Polym. Bull. (Berlin)* **1983**, *9*, 260.
(27) Popli, R.; Glotin, M.; Mandelkern, L. *J. Polym. Sci., Polym. Phys. Ed.* **1984**, *22*, 407.
(28) Flory, P. J.; Yoon, D. Y.; Dill, K. A. *Macromolecules* **1984**, *17*, 868.
(29) Tadokoro, H.; Chatani, Y.; Yoshihara, T.; Tahara, S.; Murahashi, S. *Makromol. Chem.* **1964**, *73*, 109.

The Microstructure of Block Copolymers Formed via Ionic Interactions†

T. P. Russell*

IBM Research, Almaden Research Center, 650 Harry Road, San Jose, California 95120-6099

R. Jérôme, P. Charlier, and M. Foucart

Laboratory of Macromolecular Chemistry and Organic Catalysis, University of Liège, 4000 Liège, Belgium. *Received October 6, 1987; Revised Manuscript Received December 7, 1987*

ABSTRACT: The morphology produced by solution cast mixtures of telechelic polymers end capped with tertiary amine functionalities with telechelic polymers terminated with either sulfonate or carboxylate moieties closely resembles that seen in block copolymers formed by covalent bonding of two dissimilar chain segments. It has been found by temperature-dependent small-angle X-ray scattering and optical microscopic studies that the sulfonate/tertiary amine associations are more stable at elevated temperatures than the carboxylate analogs. These effective block copolymers undergo a classic order/disorder transition at elevated temperatures similar to that seen in covalently bonded block copolymers. However, due to the nature of the ionic associations, as the order/disorder is approached, the width of the interface between the two phases remains sharp. Finally, by increasing the molecular weight of the telechelic polymers at temperatures above the order/disorder transition temperature, the effects of an upper critical solution temperature are seen. Here, the telechelic polymers appear to phase separate in a spinodal manner. The phase diagrams for these systems are dictated by the relative positions of the microphase separation temperature of the effective block copolymers, the upper critical solution temperature of the dissociated telechelic polymers, the temperature at which the ionic aggregates dissociate, and the glass transition temperature.

Introduction

The miscibility of two homopolymers is more the exception than the rule. Typically, phase separation exhibited by two polymers occurs on a size scale of several microns which gives rise to opacity and can cause a deterioration of properties due to poor interfacial adhesion. These problems can be circumvented to some extent by copolymerizing the desired monomers. Copolymerization tends to make the two polymers more miscible by covalently linking the otherwise incompatable polymers, and it also limits the microphase separation to a size scale comparable to molecular dimensions.[1] An alternate approach to the copolymerization route is to place proton donating end groups on one polymer and proton accepting moieties on the other homopolymer.

Previously, the phase separation of two immiscible polymers was modified by ionic interactions via a proton transfer from the acid end groups of one polymer to the tertiary amine end groups of a second polymer.[2] Infrared spectroscopic studies showed that proton transfer from carboxylic acid end groups to the dimethylamino end groups occurred with formation of ammonium carboxylate ion pairs.[2,3] The solution viscosity of the related telechelic polymer blends in a common, nonpolar solvent was also significantly modified by the ionic bonding between the two polymers and possible electrostatic interactions of the ammonium carboxylate ion pairs.[3] Optical microscopy has shown it is possible to obtain homogeneous mixtures on a scale of ca. 0.2 μm, depending on the nature, molecular weight, and functionality of the immiscible polymers, and the strength of the ion pairs (ammonium carboxylates or sulfonates).[3] Finally, two distinct glass transition temperatures (T_g) for the acid and tertiary amine telechelic polymer mixtures were observed which indicated that these mixtures are actually microphase separated in a manner that is analogous to block copolymers.[3] These results strongly suggest that mixtures of the acid and tertiary amine telechelic polymers form essentially a multiblock copolymer in the bulk where phase separation is restricted to the molecular level.

In this paper small-angle X-ray scattering (SAXS) studies on mixtures of amine-terminated polyisoprene with carboxylic acid terminated poly(α-methylstyrene) will be presented. It is shown that the morphologies of these

†The work reported herein was partially done at Stanford Synchrotron Radiation Laboratory which is supported by the Department of Energy of Basic Energy Sciences and the National Institute of Health, Brotechnology Resource Program, Division of Research Resources.

0024-9297/88/2221-1709$01.50/0

mixtures closely mimic that seen in multiblock copolymers. The microphase-separated structures formed by these polymers at low temperatures is also shown to undergo a disordering process at elevated temperatures similar to that seen in diblock copolymers. Upon dissociation of the ionic interactions the mixture of the homonopolymeric constituents phase separates.

Experimental Section

Telechelic polymers were prepared by anionic polymerization. Pure and carefully dried monomers and solvents were used. α-Methylstyrene and isoprene were dried over CaH_2 at room temperature and distilled under reduced pressure just prior to use. Isoprene was mixed with *n*-butyllithium and again distilled before polymerization. Polymerization was performed in previously flamed and nitrogen-purged flasks equipped with rubber septums. Hypodermic syringes and stainless-steel capillaries were used to handle liquid products under a nitrogen atmosphere. α-Methylstyrene sodium tetramer was used as a difunctional initiator, and polymerizations were performed in tetrahydrofuran THF at −78 °C. The living macrodianions were deactivated by anhydrous carbon dioxide, propanesultone, and 1-chloro-3-(dimethylamino)propane to form the α,ω-dicarboxylic acid, the α,ω-disulfonic acid, and the α,ω-bis(dimethylamino) derivatives of polyisoprene, respectively.[4] The microstructure of the polyisoprene was determined to be a mixture of 3,4/1,2 in a ratio of 65/35. Molecular weights of the telechelics were controlled by adjusting the monomer to catalyst molar ratio. The polydispersity (M_w/M_n) of the telechelics was near 1.15, and the functionality of each was greater than 1.9. The functionality was determined from M_n as determined by vapor pressure osmometry and potentiometric titration of the acid end groups with tetramethylammonium hydroxide. Titration of the dimethylamino end groups was performed with *p*-toluenesulfonic acid in a 9/1 benzene/methanol mixture. Polyisoprene was carefully stabilized by an antioxidant (Irganox 1010).

Polymer blends were prepared by solvent-casting techniques. Separate solutions of each polymer in toluene were prepared. One solution was then slowly added to the other under vigorous stirring. After the desired volumes were mixed, the solutions were allowed to stir for an additional 2 h prior to casting. Films were prepared by slow evaporation of the toluene followed by vacuum drying to constant weight at 50 °C.

Small-angle X-ray scattering studies were performed at the Stanford Synchrotron Radiation Laboratory on Beamline I-4. X-rays emanating from the storage ring first impinged on a bent, 50-cm Pt-coated, float glass mirror tilted at 17 mrad with respect to the incident beam that focused the beam in the vertical plane. Following this the beam was focused in the horizontal plane with a bent, asymmetrically cut Si(111) monochromator. Between the sample and the monochromator parasitic scattering was removed by two sets of guard slits. Monitors directly before and after the specimen monitored the incident beam flux and the attenuation factor of the sample during the course of a measurement. The detector, situated ca. 50 cm from the sample, was a self-scanning photodiode array detector containing 1024 pixels, each 25 μm × 1 mm in size. Readouts from the pixels were processed with CAMAC electronics and stored on hard disc for later use. Specimens were mounted into 6-mm brass rings with two 12-μm sheets of Kapton (Du Pont polyimide) as windows. These cells were mounted into a Mettler FP85 that controlled the temperature and allowed the beam to pass unhindered. Detailed descriptions of the facility can be found elsewhere.[5,6]

Results and Discussion

The effect that ionic interactions between the end groups of two immiscible polymers can have on the morphology has been discussed previously.[1,2] Optical microscopic observations have shown that the size of the phases formed depends on the molecular weight (M) and functionality the telechelic polymers. Morphologies ranging from coarsely phase separated mixtures with phases 20 μm or more to finely dispersed mixtures with phases <0.2 μm were found. Representative mixtures have been selected for an in-depth characterization by SAXS.

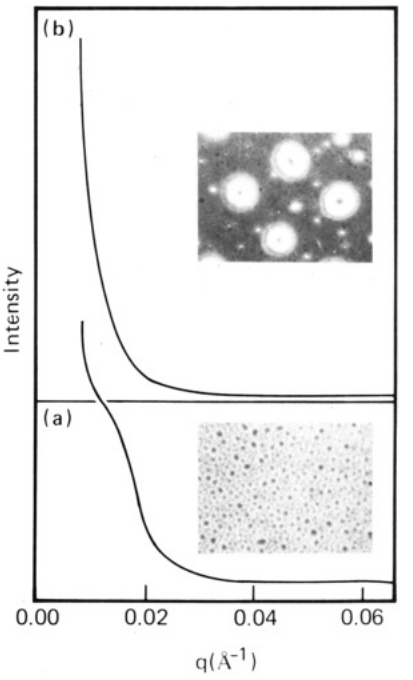

Figure 1. Small-angle X-ray scattering profiles shown as relative intensity as a function of the scattering vector **q** for mixtures of $PIP(NR_2)_2$-20K with difunctional $PS(COOH)_2$-30K (a) and monofunctional PS(COOH)-25K (b). The effect of the difunctional termination inducing a microphase separation is seen by the shoulder in the scattering profile whereas a coarse phase separation is seen for the monofunctional terminated polymer. The accompanying micrographs show that from solution cast films both mixtures exhibit a macroscopic phase separation. In the monofunctional case the texture is more coarse. The domains in the monofunctional case correspond to ca. 20 μm whereas those for the difunctionally terminated polymers correspond to ca. 1 μm in size.

In Figure 1 are shown the scattering profiles and optical micrographs of α,ω-bis-(dimethylamino)-polyisoprene (M = 20 000; $PIP(NR_2)_2$-20K) with monofunctionally and difunctionally terminated polystyrenes. The mixtures with the difunctional polystyrene (M = 30 000; $PS(COOH)_2$-30K) exhibit a phase separation on two different size scales. First, as seen in the micrograph in Figure 1a, a periodic interconnected structure reminiscent of a mixture that has undergone spinodal phase separation is observed. The characteristic spacing in this micrograph is on the order of several microns. The SAXS profile in Figure 1a, on the other hand, clearly shows the appearance of a shoulder that occurs near 500 Å with an intense zero angle component. The scattering profiles are given as relative intensity as a function of the scattering vector $q = 4\pi/\lambda \sin(\epsilon/2)$ where λ is the wavelength and ϵ is the scattering angle. Thus, it is evident from these data that mixture contains microphase-separated regions similar to a multicomponent block copolymer, but this is not distributed uniformly throughout the sample since there are concentration fluctuations on the micron size scale. The larger size scale of phase separation could be a result of the solution-casting process and is being investigated further. Mixtures of the $PIP(NR_2)_2$-20K with monofunctional polystyrene (M = 25 000; PS(COOH)-25K) exhibit dramatically different behavior. The micrograph in Figure 1b shows that a very coarse phase separation has occurred, and the SAXS profiles show no evidence for a microphase separated structure. Thus, despite the fact that the polymers would be expected to form essentially triblock copolymers and exhibit a microphase separation characteristic of this type

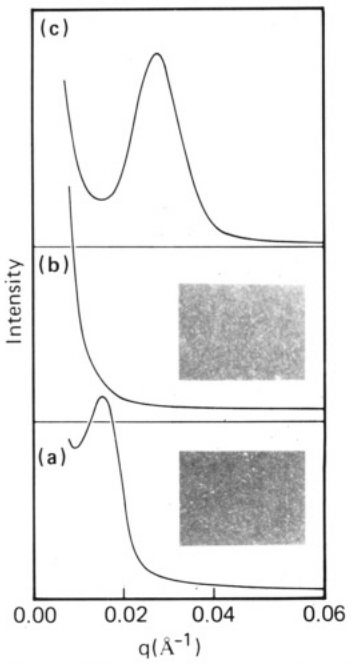

Figure 2. Small-angle X-ray scattering profiles of mixtures of $PIP(NR_2)_2$-20K with $P\alpha MSt(COOH)_2$ where the molecular weights of the latter are 5000 (b), 10 000 (a), and 15 000 (c). The dramatic effect of molecular weight on the extent of microphase separation is clearly see here.

of copolymer, such behavior is not observed. This may reflect the formation of miscelles in solution that are carried over into the bulk during solvent evaporation. These two results clearly show that in order to produce the desired microphase-separated structure from solution cast films, bifunctionally terminated telechelics are necessary.

$PIP(NR_2)_2$-20K was also blended with α,ω-dicarboxylic acid poly(α-methylstyrene) [$P\alpha MSt(COOH)_2$] of varying molecular weights. Provided the molecular weight of the $P\alpha MSt(COOH)_2$ was less than 2×10^4, optical microscopic observations showed that the mixtures were homogeneous down to the submicron level. However, for molecular weights greater than this a coarse phase separation was found.[2,3] Due to the size scale of phase separation these mixtures were not investigated by SAXS. Although indistinguishable by optical microscopy, mixtures of the $PIP(NR_2)_2$-20K with $P\alpha MSt(COOH)_2$ where the molecular weights of the latter were 5000 (-5K), 10 000 (-10K), and 15 000 (-15K) exhibited dramatic differences by SAXS. Increasing the molecular weight of the $P\alpha MSt$ effectively increases the volume fraction of the $P\alpha MSt$ from 0.2 to 0.33 to 0.43, respectively. By varying the concentration of one of the components in a copolymer, the phase diagram is effectively being traversed. In the strong interaction limit[7] the 20% copolymer would be on the verge of the spherical to cylindrical morphology transition whereas a cylindrical morphology would be expected for the 33% mixture and lamellar for the 43%. The scattering profiles shown in Figure 2 clearly reflect these changes. The scattering profile for the 20% $P\alpha MSt(COOH)_2$ mixture is given in Figure 2b. As can be seen, the intensity monotonically decreases as a function of the scattering vector characteristic of a spherical morphology where the spheres are randomly arranged in space. In Figure 2a the SAXS for the 33% $P\alpha MSt(COOH)_2$ reveals a pronounced scattering maximum occurring near a Bragg spacing corresponding to the peak maximum at 400 Å. Without the appearance of higher order reflections it is not possible from these data alone to discern whether the structure is

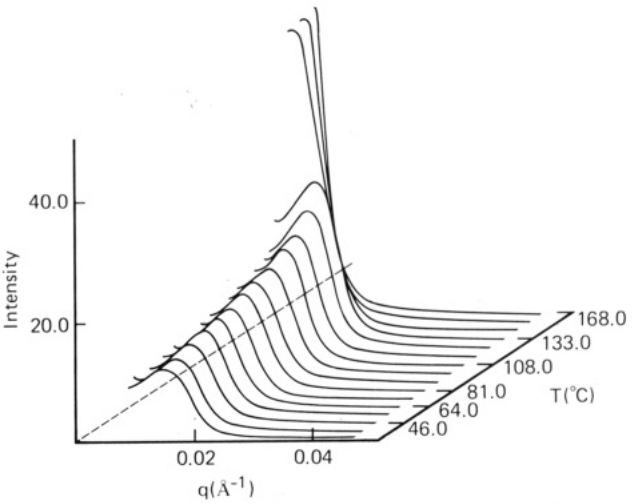

Figure 3. Temperature dependence of the SAXS at a scanning rate of 10 °C/min for a solution cast mixture of $PIP(NR_2)_2$-20K with $P\alpha MSt(COOH)_2$-10K.

cylindrical or lamellar. Similarly, the SAXS for the 43% mixture (Figure 2c) exhibits a sharp reflection at 250 Å. The fact that the long period or the repeat period for the 43% mixture has decreased from that of the 33% mixture strongly suggests that the microphase separated morphology has changed from a cylindrical to lamellar morphology. Had the morphology remained constant an increase in the period would have occurred.

The temperature dependence of scattering profiles have been analyzed for various blends of $PIP(NR_2)_2$-20K and $P\alpha MSt(COOH)_2$. Figure 3 show the variation in the SAXS for the diamine mixtures with $P\alpha MSt(COOH)_2$-10K from 25 to 170 °C at a scanning rate of 10 °C/min. As can be seen the scattering maximum shifts to smaller angles, i.e., the long period increases, and eventually disappears at higher temperatures. An increase in the long period would be expected from thermal expansion of the individual phases. This, however, amounts to only an 8% increase in the long period which is far too small to explain the observed changes. A more plausible explanation is that as the temperature is increased the mobility of the molecules increase, the phases become more pure and the system undergoes a phase transitions from lamellar to cylindrical to spherical morphologies. At the highest temperatures the ionic associations of the carboxy and the tertiary amine groups are disrupted and the systems behave as a mixture of two homopolymers and phase separation ensures. Major changes in the scattering profiles occur near 140 °C which, if the $P\alpha MSt$ phase contained some PIP, would correspond to the glass transition temperature of the $P\alpha MSt$ rich phase.

It is interesting to examine the temperature dependence of the total integrated scattering or invariant, Q, and the width of the phase boundary, E, between the $P\alpha MSt$-rich and PIP-rich phases as determined from a Porod analysis of the high-angle scattering data.[8,9] At room temperature, as shown in Figure 4 $E \simeq 40$ Å. Up to 140 °C E increases gradually, then decreases precipitously. The increase in E has several origins. First, there is an increase in the motion of molecules across the interface to enhance phase purity. At equilibrium this would not give rise to an increase in E. However, the $P\alpha MSt$ rich phase is near its T_g, and the molecular mobility is slower than the time scale of the measurement. Increasing temperature will weaken the ionic associations of the carboxy and tertiary amine groups, thereby broadening the width of the interface where these interactions primarily occur. The sudden drop

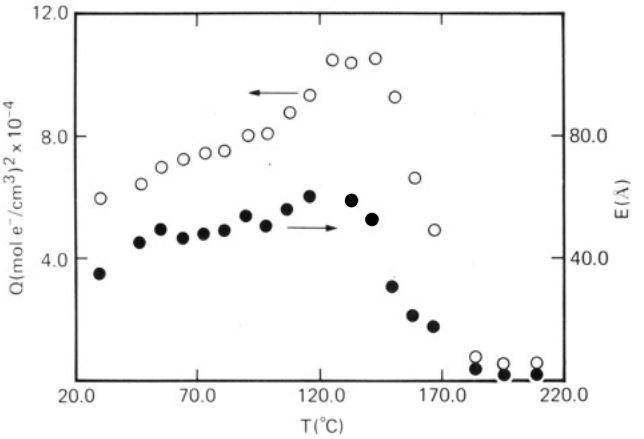

Figure 4. Total integrated scattering or invariant Q (○) and the width of the diffuse phase boundary E (●) as a function of temperature. These parameters were derived from the scattering profiles shown in Figure 3.

in the diffuse boundary can only be explained by a coarse phase separation of the telechelic polymers, i.e., the ionic interactions at these temperatures are not strong enough to hold the telechelic polymers together as an effective block copolymer. This essentially breaks the copolymer into the individual homopolymer constituents and results in phase separation. A simple transition of the morphology from cylindrical to spherical would not result in the observed drop in E.

The temperature dependence of Q parallels that of E. To understand this we must examine the different contributions to Q. The invariant for a two phase system is given by

$$Q = \phi_1\phi_2(\rho_1 - \rho_2)^2 \tag{1}$$

where ϕ_i is the volume fraction of phase i with electron density ρ_i. The total derivative of Q with respect to temperature is given by

$$dQ = [\phi_1\phi_2^2(\rho_1 - \rho_2)^2(\alpha_1 - \alpha_2) + \phi_1^2\phi_2(\rho_1 - \rho_2)^2 \times (\alpha_2 - \alpha_1) + 2\phi_1\phi_2(\rho_1 - \rho_2)(\alpha_2\rho_2 - \alpha_1\rho_1)]\, dT \tag{2}$$

where α_i is the thermal expansion coefficient of phase i. Therefore, Q_{T_2}, the invariant at a temperature T_2, in terms of Q_{T_1}, the invariant at a temperature T_1, is given by

$$Q_{T_2} = Q_{T_1}\left\{1 + \left[(\alpha_1 - \alpha_2)(\phi_2 - \phi_1) + 2\left(\frac{\alpha_2\rho_2 - \alpha_1\rho_1}{\rho_1 - \rho_2}\right)\right]\Delta T\right\} \tag{3}$$

These equations assume that the purity of the phases remain constant as a function of temperature. For the two components of interest, PαMSt and PIP, a value of Q at 25 °C equal to 7.53×10^{-4} (mol e/cm^3)^2 would be expected. Experimentally a value of 5.7×10^{-4} (mol e/cm^3)^2 is found. Thus, it is apparent that the two phases are not comprised of pure PαMSt and PIP. Equation 3 would predict that below the T_g of the PαMSt phase an increase in Q would be expected from the thermal expansion coefficient. Above the T_g of the PαMSt phase the increase in Q would be less pronounced. This is not observed experimentally, and, therefore, the concentrations of the PαMSt and PIP in the phases must be changing with temperature. However, the change must be such that the PαMSt-rich phase gets richer in PαMSt. Using eq 3 a value of Q at 150 °C, assuming pure PαMSt and PIP phases, is 1.32×10^{-3} (mol e/cm^3)^2. Experimentally, Q is found to be 1.15×10^{-3} (mol e/cm^3)^2. A comparison of the 25 and 150 °C experimental and calculated values clearly shows that the two phases have become richer in the individual components.

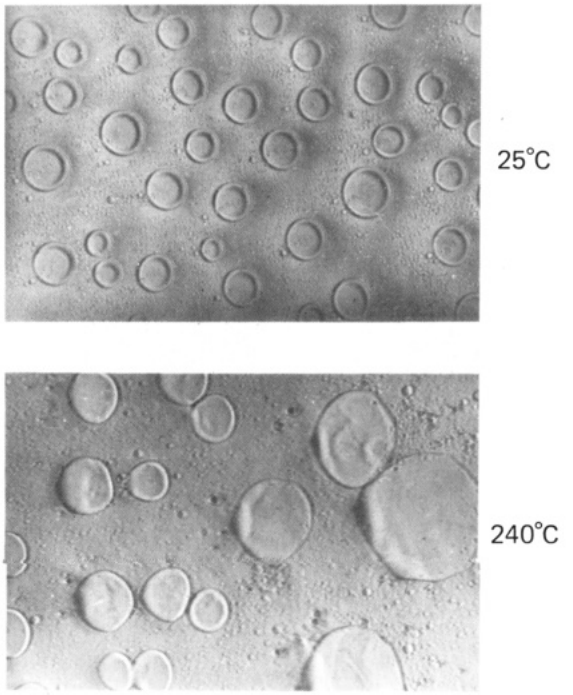

Figure 5. Optical micrographs of nonfunctionalized mixtures of PIP-27K with PαMSt-14K as cast from solution (a) and heated to 240 °C (b). Coarse phase separation as indicated by the 10 μm domains in (a) and 20 μm domains in (b) are evident. Heating only brings about an increase in the size scale of the domains. Immiscibility is seen over the entire temperature range.

The invariant, theoretically, is independent of the size and shape of the scattering entities provided the scattering occurs at angles that can be resolved experimentally. If, at 100 °C, the system underwent a morphological transition from a cylindrical to spherical morphology, then, according to calculations, sufficient scattering would have been observable to obtain a reliable value of the invariant. Consequently, the drop in Q can only be explained by changing the size of the scattering moieties such that the resultant scattering occurs at angles beyond the resolution limits. This, without question, points to a macroscopic phase separation as indicated previously.

Although no direct observation is available, the sharp transition from a regular phase structure to a coarsely phase separated system is most likely due to a breakup of the ion pairs with formation of the individual acid and tertiary amine end groups. In keeping with this view, it must be mentioned that nonfunctionalized PIP(M_w = 27 000) and PαMSt(M_w = 14 000) are completely immiscible over the temperature range from 25 to 240 °C as illustrated by the micrographs in Figure 5. Once these polymers are end-functionalized by amine and carboxylic acid groups, respectively, the related blends appear homogeneous down to the submicron level. Incipient phase separation occurs when the mixtures are heated to 175 °C for 15 min and rapidly quenched to 25 °C for microscopic observation. This is clearly evident from the micrographs in Figure 6. A much coarser phase separation occurs when the previous thermal treatment is repeated to 225 °C.

Since the mesophase structures formed by the ammonium carboxylates are disrupted at high temperatures, ammonium sulfonates, which form stronger ionic associations, were prepared to stabilize the organized phase morphology well beyond the T_g of PαMSt domains. Two blends have been considered on the basis of a PIP similar to that used previously, i.e., PIP(NR$_2$)$_2$-18K and α,ω-di-

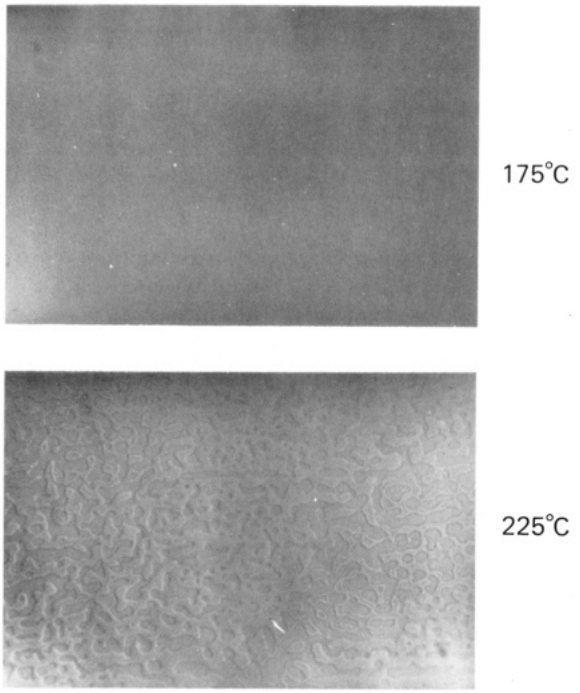

Figure 6. Optical micrographs of mixtures containing functionally terminated PIP$(NR_2)_2$-20K with PαMSt$(COOH)_2$-10K at 175 and 225 °C. As can be seen in (a) the mixtures are homogeneous down to the submicron level prior to heating to 225 °C whereupon (b) a coarse phase separation with domains of 2–5 μm in size is evident. The appearance of the domain structure in (b) resembles that seen in mixtures that have phase separated via a spinodal mechanism.

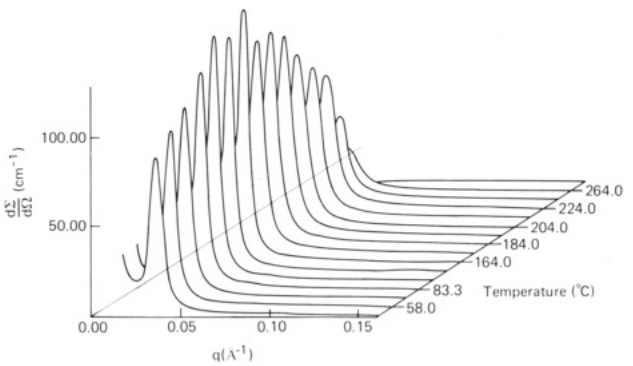

Figure 7. Temperature dependence of the SAXS from a mixture of PIP$(NR_2)_2$-18K with PαMSt$(SO_3H)_2$-8K at a scanning rate of 10 °C/min.

sulfonic acid PαMSt with molecular weights of 8000 and 14 000. Figure 7 illustrates the temperature dependence of the SAXS profile for the PIP$(NR_2)_2$-18K/PαMSt-$(SO_3H)_2$-8K blend. The results, reported in absolute, units show a well-resolved maximum occurring at a Bragg spacing of 170 Å at room temperature. The SAXS profiles become much more clearly resolved, i.e., sharper and more intense, as the temperature is increased, reaching a maximum near 165 °C. At higher temperatures, the reflection diminishes in intensity and becomes somewhat broader until disappearing near 260 °C. A very weak and broad third-order reflection is found at room temperature that does not sharpen at elevated temperatures. The Bragg spacing corresponding to the position of the maximum is shown in Figure 8. It is clear from these data that the periodicity in the phase morphology does not change dramatically. If anything, above 100 °C a slight decrease in the spacing is found, and then, near 180 °C, the spacing begins to gradually increase. The spacing is, however,

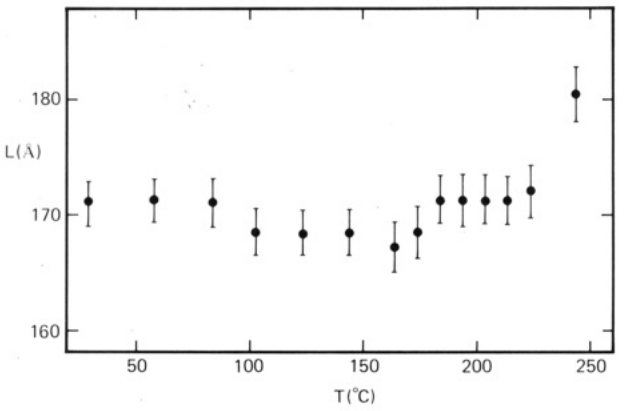

Figure 8. Temperature dependence of the long period for a mixture of PIP$(NR_2)_2$-18K with PαMSt$(SO_3H)_2$-8K at a scanning rate of 10 °C/min. The long periods shown correspond to Bragg spacing derived from the position of the peak maxima of the SAXS profiles in Figure 7.

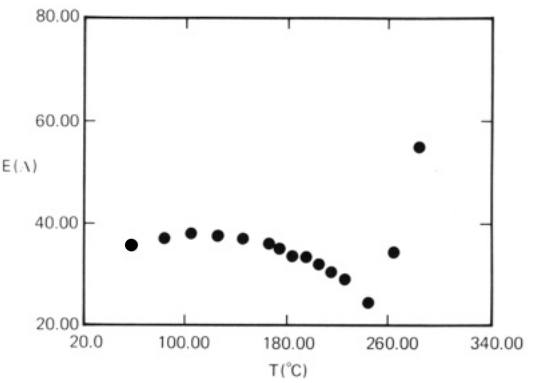

Figure 9. Width of the diffuse phase boundary determined from the scattering profiles in Figure 7 as a function of temperature.

maintained up to ca. 225 °C at which point a dramatic increase is seen. Paralleling this increase, the intensity drops off indicating the introduction of a disordering. A very interesting result is shown in Figure 9. The thickness of the diffuse phase boundary is found to remain relatively constant up to ca. 160 °C and then begins to decrease with increasing temperature reaching a minimum near 230 °C. Increasing the temperature further causes a dramatic increase in the E. In comparison to the carboxy/tertiary amine mixtures the interface formed by the sulfonate/tertiary amine mixtures is nearly 50% smaller and has a much weaker temperature dependence. These results would indicate that a more well-defined morphology is formed by the sulfonate terminated telechelics. The decrease seen near 160 °C parallels the slight increase observed in the long period and suggests that at this temperature the mobility of the molecules is sufficiently high enough to enhance the order in the system. The sudden increase in E near 230 °C again corresponds to the dramatic change in the long period strongly supporting the suggestion that the ionic associations are disrupted and a coarse phase separation ensues.

The variation in Q with temperature for the PIP-$(NR_2)_2$-18K/PαMSt$(SO_3H)_2$-8K mixtures is given in Figure 10. If the PIP and PαMSt microphases were pure neglecting the effect of the sulfonate group, then Q is calculated to be 8.11×10^{-4} (mol e/cm^3)^2 at 25 °C. Experimentally a value of 8.6×10^{-4} (mol e/cm^3)^2 is found which, while slightly larger than the predicted value, shows that the PIP and PαMSt are essentially fully microphase separated consistent with the lower values of E found for these mixtures. Using eq 3 the invariant at 180 °C is calculated

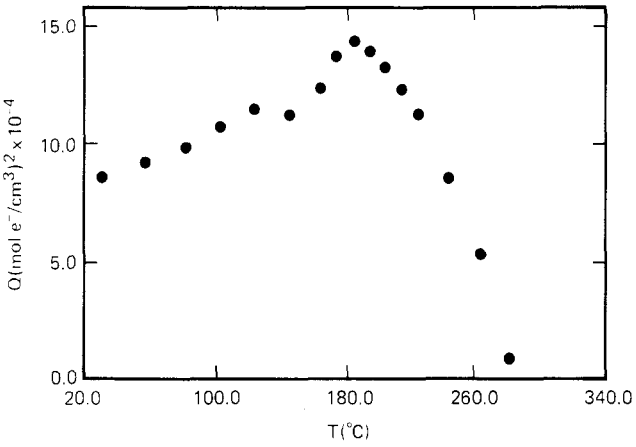

Figure 10. Total integrated scattering Q as a function of temperature for the data shown in Figure 7.

to be 1.32×10^{-3} (mol e/cm^3) which is, to within experimental errors and assumptions made, identical with the value of 1.45×10^{-3} (mol e/cm^3) found experimentally. Therefore, the continuous rise in Q up to ca. 180 °C can be explained simply by the thermal expansion of the phases and complete microphase separation of the mixture into PαMSt and PIP phases.

Near 180 °C the invariant is seen to decrease sharply with temperature. Given that the long period remains virtually constant and the invariant decreases, it can only be concluded that the effective copolymer is approaching an order/disorder transition. This phenomenon has been described by Leibler[1] and has been experimentally observed by several independent researchers.[10-13] What is unusual about this copolymer formed by ionic associations is that the ionic associations maintain a sharp interface while approaching the order/disorder transition. Typically when phases mix, it would be expected that the phase boundary would broaden as the disorder transition is approached. While it is clear from the drop in Q that phase mixing is occurring, the phase boundary is maintained narrow in these effective block copolymers. At present it is not clear what gives rise to this behavior. At ca. 260 °C, the pronounced scattering vanishes, the diffuse phase boundary and the fluctuation scattering increase sharply, and Q is quite small. These results are characteristic of a homogeneous mixture and are consistent with differential thermal analysis of the blend where a sample annealed at 250 °C for 30 min shows only one T_g at 12 °C. The disordering of the microphase morphology, however, cannot be attributed to the transformation of the ion pairs into individual acid and tertiary amine end groups, respectively. If this were the case, the PαMSt and PIP chains would phase separate as observed for the carboxylate system. At 260 °C and higher temperatures, thermal fluctuations prevent electrostatic interactions of the ammonium and sulfonate ion pairs and impede the formation of a well-defined microphase separated morphology. The homogeneity of the blend at high temperatures is, therefore, due to the effective copolymeric nature of the chains.

For typical block copolymers in the disordered state a diffuse scattering maximum related to the radii of gyration and molecular weights of the individual blocks and to the Flory–Huggins interaction parameter between segments of each block is predicted[1] and has been observed.[10-13] For both the PIP(NR$_2$)$_2$-18K/PαMSt(SO$_3$H)$_2$-8K and the PIP(NR$_2$)$_2$-20K/PαMSt(COOH)$_2$-5K, at elevated temperatures (as shown in Figure 2) this diffuse scattering maximum, termed the correlation hole scattering, was not evident. This may occur if the electron density difference

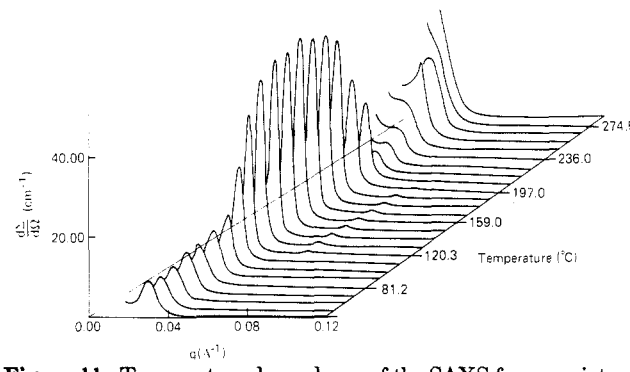

Figure 11. Temperature dependence of the SAXS from a mixture of PIP(NR$_2$)$_2$-18K with PαMSt(SO$_3$H)$_2$-14K at a scanning rate of 10 °C/min.

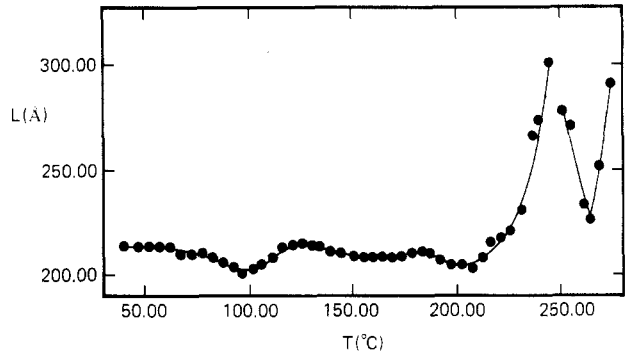

Figure 12. Long period derived from the Bragg spacing corresponding to the position of the peak maximum for the scattering profiles shown in Figure 11. Note the pronounced increase in the long period near 240 °C followed by a rapid drop at higher temperatures.

between the effective blocks is too small to be observed. It may, also, be associated with the fact that the ionic copolymers are essentially multiblock copolymers that are held together loosely in the homogeneous state by ionic interactions. Intrachain density correlations that are well-defined in a covalently bonded block copolymer are much less well-defined here. This would cause a broadening of the correlation hole maximum, thereby making the observation of this scattering difficult.

Increasing the molecular weight of the PαMSt produces pronounced changes in the temperature dependence of the small angle scattering. In Figure 11, the SAXS from a PIP(NR$_2$)$_2$-18K/PαMSt(SO$_3$H)$_2$-14K is shown as a function of temperature. A single, well-developed maximum is observed at room temperature. Normalization of the data for plotting purposes only appears to make it look small in the figure. Up to ca. 100 °C only a slight increase in the scattering is observed. Above this not only does the scattering increase enormously, but also a pronounced third order maximum, characteristic of a lamellar morphology with near 50/50 composition, emerges. Symmetry conditions cause the second-order reflections to be absent. As with the PαMSt(SO$_3$H)$_2$-8K containing blend, the intensity of the SAXS increases up to 165 °C and then begins to decrease. However, rather than vanishing at ca. 200 °C, another maximum emerges with a spacing somewhat larger than that observed at lower temperatures. This reflection is much broader and less well-defined although it is still intense. This maximum persists up to 260 °C, whereupon it shifts to scattering vectors beyond instrumental resolution. These data are quite unusual for multiphase systems and exemplifies the power of real time scattering studies using synchrotron light sources. As with the other data, these results are in absolute units. Figure 12 shows

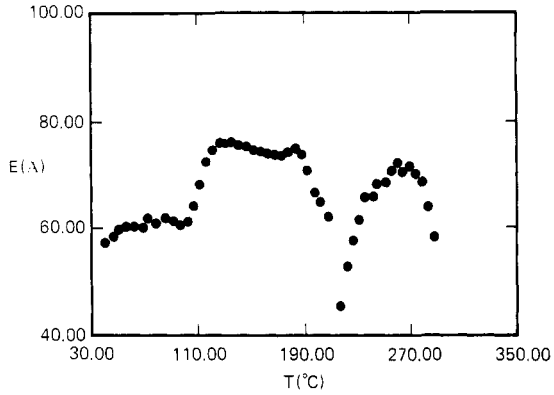

Figure 13. Width of the diffuse phase boundary E as a function of temperature for the SAXS profiles shown in Figure 11.

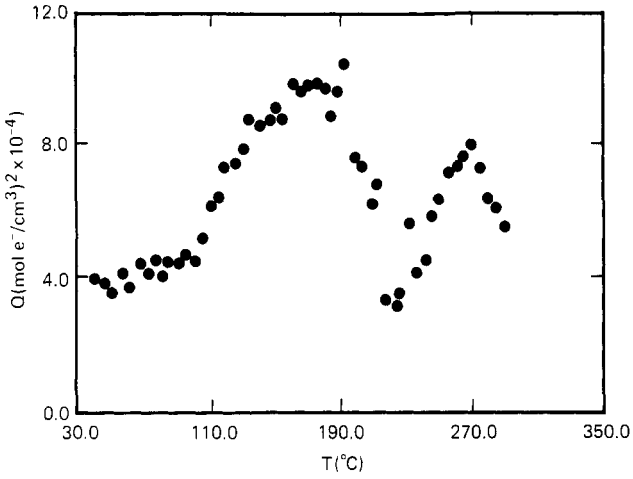

Figure 14. Total integrated scattering as a function of temperature for the scattering profiles shown in Figure 11.

the temperature dependence of the long period. As can be seen this remains relatively constant at an average value of 210 Å up to 200 °C. Two shallow minima are, however, observed at 100 and 200 °C, i.e., at temperatures where the reflection starts increasing dramatically and where it begins to disappear, respectively. Beyond 200 °C, the long period increases enormously, and suddenly, at 245 °C, it decreases sharply up to 265 °C. Thus, over the temperature range where a SAXS reflection is clearly observed, the long period passes through a very sharp maximum. Finally, it increases again sharply until the spacing is no longer observable.

The variation in the diffuse phase boundary, E, and the invariant Q parallel the changes observed in the long period. As shown in Figure 13 up to ca. 100 °C, E remains relatively constant at 60 Å whereupon it increases rapidly by 25% to 75 Å, and E then remains unchanged to 180 °C where it suddenly goes through a sharp drop to ca. 45 Å. As the temperature is increased, further E increases rapidly, reaching a maximum value of ca. 75 Å near 260 °C and then decreases again. Similarly, the invariant shown in Figure 14 gradually increases up to 100 °C, then increases sharply up to ca. 180 °C, whereupon it goes through a pronounced minimum and is followed by another rapid increase and decrease near 260 °C.

The combination of these results at first appears somewhat contradictory in that as Q increases, a decrease in E would be expected. However, clarification of these apparent discrepancies becomes obvious when the magnitudes of Q are examined. As stated previously, for a two-phase system comprised of PαMSt and PIP phases at 25 °C a value of $Q = 7.53 \times 10^{-4}$ (mol e/cm^3)^2 would be expected. Experimentally a value of 4×10^{-4} (mol e/cm^3)^2 is found clearly showing that, as cast, the individual phases are not pure PαMSt or PIP. Due to this, the glass transition temperature of the PαMSt phase is reduced to ca. 100 °C. Up to 100 °C, thermal expansion can account for the observed changes. At ca. 100 °C, there is sufficient mobility in the system to allow the polymers to microphase separate further. The extent to which this happens depends upon the temperature of the measurement since this will control the T_g of the PαMSt phase. This will also give rise to the broader phase boundary. At 180 °C the measured value of Q is 1.15×10^{-3} (mol e/cm^3)$_2$ which using eq 3 compares well to the value of 1.32×10^{-3} (mol e/cm^3)^2 calculated assuming pure phases. Consistent with this result is the sharpening of the scattering profiles and the appearance of a third-order reflection. Increasing the temperature further causes Q and E to drop, but the long period remains virtually constant and the scattering profiles become more diffuse. As with the PαMSt$(SO_3H)_2$-8K mixtures these changes can only be described by the approach of the system to an order/disorder transition. Consistent with the PαMSt$(SO_3H)_2$-8K results, the diffuse phase boundary does not broaden but sharpens which, as stated before, must be attributed to the ionic associations rather than covalent bonding of consecutive blocks. In contrast to the PαMSt$(SO_3H)_2$-8K mixtures the SAXS of the 14K mixtures shows the effects of this order/disorder transition at lower temperatures. This is, also, inconsistent with the order/disorder transition behavior observed in covalently bonded block copolymers since an increase in the molecular weight would be expected to raise the transition temperature and results, most likely, from the reduction in the extent of ionic interactions in the system.

At elevated temperatures the PαMSt$(SO_3H)_2$-14K mixtures would be expected to exhibit scattering characteristic of a disordered copolymer. Rather, the SAXS shows the development of a scattering maximum that increases in intensity and shifts to smaller scattering vectors. These data, therefore, show that the system is undergoing a phase separation, very much like a spinodal phase separation, that is characteristic of a homopolymer mixture below an upper critical solution temperature (UCST) or above the lower critical solution temperature. Studies of mixtures of polystyrene with polybutadiene,[14,15] which closely resemble a mixture of the constituent telechelic polymers under investigation in this study, would argue in favor of an UCST. Consequently, the ionic associations of the $-SO_3^-$ and $-NHR_2^+$ are not strong enough at these temperatures to prevent the system from undergoing a coarse phase separation. It should be noted that the behavior of the PαMSt$(SO_3H)_2$-8K mixtures is different in that a coarse phase separation was not observed. Thus, the order/disorder transition must occur at temperatures either above the UCST; i.e., the UCST is reduced by the reduction in the molecular weight, or below the temperature at which disruption of the ionic aggregates occurs.

Consequently, a unified description of the phase diagram of the telechelic copolymers arises from these studies. It is apparent that four different features have to be considered to understand the observed SAXS results. These include the mesophase separation temperature of the copolymers formed by ionic associations, the UCST of the constituent homopolymers, the temperature, T_i, at which ionic associations are disrupted, and the glass transition temperature T_g. The relative position of these will dictate the morphology. Three such examples are shown in Figures 15, 16, and 17 for the PIP$(NR_2)_2$-18K/PαMSt-$(COOH)_2$-10K, PIP$(NR_2)_2$-18K/PαMSt$(SO_3H)_2$-8K, and

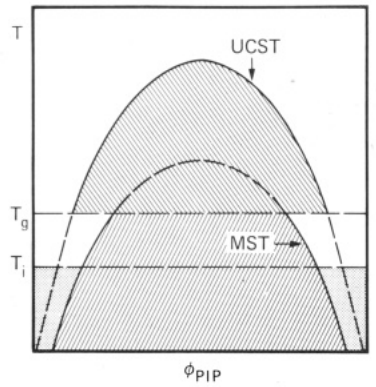

Figure 15. Proposed phase diagram for the PIP$(NR_2)_2$-18K/PαMSt$(COOH)_2$-10K telechelic mixtures where UCST is the upper critical solution temperature of the constituent telechelic polymers, MST is the microphase separation temperature of the ionic copolymers, T_g is the glass transition, and T_i is the temperature at which the ionic associations forming the block copolymers are disrupted. The left to right diagonally hatched area is where the mixtures exhibit a microphase-separated morphology similar to that seen in covalently bonded block copolymers. The right to left diagonally hatched area is where the mixtures phase separate in a manner analogous to simple homopolymer mixtures. The stippled area is where the mixtures exist as a disordered copolymer phase, and the clear area is where the mixture is a homogeneous mixture of the constituent telechelics. The dashed lines are continuations of the phase diagrams which due to ionic aggregation or disruption of the end groups are not possible to observe.

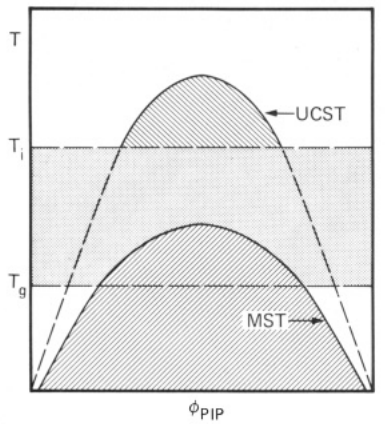

Figure 16. Schematic phase diagram of the PIP$(NR_2)_2$-18K/PαMSt$(SO_3H)_2$-8K telechelic mixtures. This figure is labeled in a manner similar to Figure 15.

PIP$(NR_2)_2$-18K/PαMSt$(SO_3H)_2$-14K mixtures, respectively.

In Figure 15, $T_i < T_g$, the MST < UCST, and the T_g is less than the maximum of the MST. If a 33% concentration of PIP is examined, which corresponds to the PIP$(NR_2)_2$-18K/PαMSt$(COOH)_2$-10K mixture, as a function of temperature it is seen that at low temperatures a microphase separated morphology is found. As the temperature is increased, T_i is exceeded but the system is still below T_g. Thus, the microphase separated morphology is frozen in. Increasing the temperature above T_g, the components of the copolymer behave as individual homopolymer molecules below the UCST and coarse phase separation ensues.

For the PIP$(NR_2)_2$-18K/PαMSt(SO_3H)-8K $T_i > T_g$ and the UCST > MST. In addition $T_g <$ MST and MST < $T_i <$ UCST. At low temperatures, as seen in Figure 16, a 30% PIP mixture would be below the MST and a microphase-separated morphology is seen. Increasing the temperature above the T_g and eventually the MST induces the order/disorder transition, and a uniform melt is observed. At higher temperatures, i.e., greater than T_i, the effective homogeneous copolymer melt is broken up into the constituent homopolymers and phase separation of the homopolymers occurs.

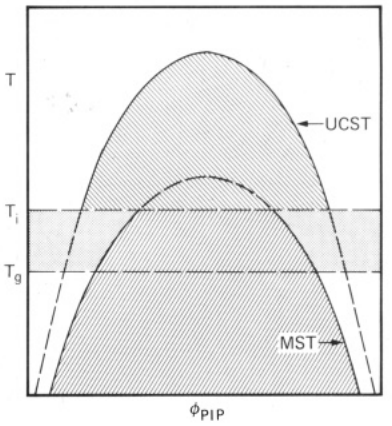

Figure 17. Schematic phase diagram of the PIP$(NR_2)_2$-18K/PαMSt$(SO_3H)_2$-14K telechelic mixtures. The labeling is the same as in Figure 15.

Finally, the phase diagram for the PIP$(NR_2)_2$-18K/PαMSt$(SO_3H)_2$-14K mixtures is shown in Figure 17. Here, MST < UCST, $T_g < T_i$, and $T_i <$ MST. Thus, for a 44% PIP concentration at low temperatures a microphase-separated morphology is seen. Upon heating above T_g this morphology is maintained until T_i is reached. At this point the copolymer nature of the system is lost and the telechelics phase separation in the normal homopolymer fashion.

In conclusion, it has been shown for the first time that the morphology developed by mixtures of telechelic polymers end capped with tertiary amine functionalities with telechelic polymers terminated with either carboxylate or sulfonate end groups closely resembles that seen in covalently bonded block copolymers. Wilkes has recently reported similar behavior when a dimethylamino-terminated poly(tetramethylene oxide) is quarternized by a dibenzyl halide.[16] It is also evident that the sulfonate groups form stronger ionic associations with the tertiary amino groups than the carboxylate moieties as evidence by the temperature dependence of the SAXS. At elevated temperature these effective copolymers appear to undergo a classic order/disorder transition characteristic of block copolymers. In contrast to the covalently bonded block copolymers the width of the interface remains sharp in these copolymers formed by ionic associations as the order/disorder transition is approached. In addition, the well-known correlation hole scattering characteristic of the disordered state in block copolymers was not observed in these systems due most likely to the nature of the block linkages. Finally, as the molecular weight of the telechelics is increased, the effect of an upper critical solution temperature is seen and macroscopic phase separation ensues at elevated temperatures by an apparent spinodal mechanism.

Acknowledgment. R.J., P.C., and M.F. are very much indebted to SPPS (Services de la Programmation de la Politique Faentifique) for valuable support. They are grateful to Professor Teyssie for his continuing interest. P.C. and M.F. thank the "Institut pour l'encouragement de la recherche scientifique dans l'industrie et l'agriculture" (IRSIA) for a fellowship. Finally, R.J. thanks IBM World Trade Program for having awarded him a Research Fellowship to visit the Almaden Research Center (San Jose, CA, USA).

Registry No. PIP, 9003-31-0; PαMSt, 25014-31-7.

References and Notes

(1) Leibler, L. *Macromolecules* **1982**, *19*, 2621.
(2) Horrion, J.; Jérôme, R.; Teyssié, Ph. *J. Polym. Sci., Polym. Lett. Ed.* **1986**, *24*, 69.
(3) Horrion, J.; Jérôme, R.; Teyssié, Ph., in preparation.
(4) Broze, G.; Jérôme, R.; Teyssié, Ph. *Macromolecules* **1982**, *15*, 920.
(5) Stephenson, G. B. Ph.D. Thesis, Stanford University, 1982.
(6) Russell, T. P.; Koberstein, J. T. *J. Polym. Sci., Polym. Phys. Ed.* **1985**, *23*, 1109.
(7) Ohta, T.; Kawasaki, K. *Macromolecules* **1986**, *19*, 2621.
(8) Ruland, W. *J. Appl. Crystallogr.* **1971**, *4*, 70.
(9) Koberstein, J. T.; Morra, B.; Stein, R. S. *J. Appl. Crystallogr.* **1980**, *13*, 34.
(10) Bates, F. S.; Hartney, M. A. *Macromolecules* **1985**, *18*, 2478.
(11) Mori, K.; Hasegawa, H.; Hashimoto, T. *Polym. J. (Tokyo)* **1985**, *17*, 799.
(12) Roe, R. J.; Fishkis, M.; Chang, C. J. *Macromolecules* **1981**, *14*, 1091.
(13) Owens, J. N.; Koberstein, J. T.; Russell, T. P., submitted for publication in *Macromolecules*.
(14) Russell, T. P.; Hadziioannou, G.; Warburton, W. K. *Macromolecules* **1985**, *18*, 78.
(15) Russell, T. P.; Ronca, G. *Macromolecules* **1985**, *18*, 665.
(16) Wilkes, G. L., private communication.

Rotational Motion of a Homologous Series of Solvent Molecules in Amorphous Poly(methyl methacrylate). 1. Studies of the Solvents

Jung-Ki Park[†] and R. Pecora*

Department of Chemistry, Stanford University, Stanford, California 94305

A. C. Ouano[‡]

IBM Corporation, San Jose, California 95193.

Received October 9, 1987; Revised Manuscript Received December 21, 1987

ABSTRACT: The depolarized light scattering reorientation times of a series of *n*-alkyl *p*-chlorobenzoates (PCAB's) (with *n*-alkyl varying from methyl to *n*-pentyl) have been measured in the neat liquids and in 16% (vol/vol) solutions in CCl_4 at various temperatures. Densities and viscosities of the neat liquids and viscosities of the 16% solutions were also measured. Plots of the reorientation times for each homologue versus η/T both in the neat liquid and in dilute solution are well fit by straight lines with nonzero zero-viscosity intercepts. Tests of the scaling of the reorientation times with molecular length as predicted by hydrodynamic theories for reorientation of rigid rods were performed. The reorientation times of the entire series of neat PCAB's fit well to a straight line when plotted versus $\eta L^3/T(\ln \rho + \delta)$ where ρ is the molecular axial ratio and δ is the hydrodynamic end effect correction. The homologues in 16% CCl_4 solution also exhibited reorientation times that gave good linear fits when plotted versus $\eta L^3/T(\ln \rho + \delta)$. The slopes of the plots for the neat liquids and the solutions were the same within experimental error, indicating that the static and dynamic pair correlation factors are probably not important for the systems studied. The slopes of these plots are not as large as those predicted by the Tirado and Garcia de la Torre theory for rigid rods with stick boundary conditions. The major difference between the plots for the neat liquids and the CCl_4 solutions is that the zero-viscosity intercept is larger for the neat liquids.

I. Introduction

The rotational dynamics of small molecules in liquids has been a longstanding subject of study by liquid-state physicists.[1-4] Such topics as the relation between the single molecule and collective reorientation times, the anisotropy of the reorientation times, the viscosity dependence of the single molecule times, and the role of orientational correlations and strong intermolecular forces (such as hydrogen bonding) have all been investigated. Reorientation times of molecules in liquids are commonly interpreted by using hydrodynamic models. In principle, such theories are strictly applicable only to the motion of large particles immersed in a medium composed of much smaller molecules since they treat the solvent as a continuum. However, much experimental work has shown that the reorientation times of small molecules in solutions with similarly sized solvent molecules are often linear functions of the solution viscosity—an indication that hydrodynamic theories may be applicable. Even in the presence of "strong" interactions such as hydrogen bonding between solvent and solute, it has been shown that in many cases the reorientation time remains a linear function of the solution viscosity. Thus, the hydrodynamic description of reorientation in liquids appears to be more general than one might expect from the derivations of specific relations—particularly those relating reorientation times to solution viscosity.

There is a need to test hydrodynamic models of molecular reorientation for a homologous series of small, rodlike molecules in the liquid state and in solution. In addition, the influence of polymer matrices on the reorientation of small solvent molecules has been only rarely studied, although it is of great scientific and technological importance. In this paper, we study the reorientation of a homologous series of rodlike molecules, the *n*-alkyl *p*-chlorobenzoates (with *n*-alkyl varying from methyl to pentyl) in the neat liquid as well as some studies of the same molecules in 16% vol/vol solutions in CCl_4. We test the explicit molecular length dependence of the orientational relaxation times predicted by hydrodynamic models for the series of solvents. The major experimental technique used is depolarized dynamic light scattering using a Fabry–Perot interferometer as the predetection filter.[4] To aid in the interpretation of the experiments, the viscosities and densities of the series of solvents were mea-

[†] Current address: Chemical Engineering Department; Korea Institute of Technology, Taejon, Korea.
[‡] Current address: Digital Equipment Corporation, 10500 Ridgeview Court, Cupertino, CA 95014.

0024-9297/88/2221-1717$01.50/0